Articles

π^* Level Tuning in a Series of Diimine Ligands Based on Density Functional Theory: Application to Photonic Devices

G. Albano, P. Belser,* and C. Daul

Institute of Inorganic Chemistry, University of Fribourg, CH-1700 Fribourg, Switzerland

Received June 27, 2000

Energy- and electron-transfer processes are very important for artificial photosynthesis and a variety of other applications. $[(bpy)_2Ru(PAP)Os(bpy)_2]^{4+}$ and its oxidized form $[(bpy)_2Ru(PAP)Os(bpy)_2]^{5+}$ perform efficient photoinduced energy- and electron-transfer processes, respectively ($k_{en} = 5.2 \times 10^7\ s^{-1}$, $k_{el} = 7.2 \times 10^6\ s^{-1}$). The introduction of appropriate donor and acceptor units on the Ru^{2+} center can improve the lifetime of the excited state, resulting in a much longer and efficient storage of energy. Nonempirical (density functional) calculations and experimental data are used to predict the best donor and acceptor ligands for improving electron- and energy-transfer processes. Such a result can be extended to all polynuclear complexes where electronic coupling between the metal centers is very weak.

1. Introduction

Photoinduced energy and electron-transfer processes lie at the heart of many biological phenomena (e.g., photosynthesis)[1] as well as a variety of applications.[2] In the early 1970s, it was recognized that excited coordination compounds can be easily involved in bimolecular processes such as energy and electron transfer.[3] Nowadays, the interest of chemical research has shifted from mononuclear (for example, $[Ru(bpy)_3]^{2+}$) to polynuclear complexes (supramolecular systems),[4] which offer numerous advantages, such as absence of diffusional effects, well-defined geometry, distance and orientational effects, and the role of the bridging ligand.[5] Research in this area aims to develop supramolecular species capable of performing valuable photoinduced energy- and electron-transfer processes, for the construction of sensors and light harvesting and charge separation devices.[6]

Covalently linked two-component systems are the simplest class of supramolecular architecture for the study of electron- and energy-transfer processes.[7] Experiments have shown that, for their electrochemical and photophysical properties, the best active units are polypyridine complexes of Ru(II) and Os(II),[8] whereas the best connectors between the metal centers are rigid bridging ligands with a C_2-axis.[9] An example of a system that satisfies these requirements is shown in Figure 1 (L = bpy).[10] In this complex, a $Ru(bpy)_2(phen)^{2+}$ unit, the *donor*, is connected to a $Os(bpy)_2(phen)^{2+\text{ or }3+}$unit, the *acceptor*, via the PAP bridging ligand. Thanks to the geometry of the PAP ligand[11] the two chromophores remain along the same line at a fixed distance (2.1 nm) and are perpendicular each other, and the saturated spacer (the adamantane unit) in PAP breaks the electronic communication between them. Such a weak electronic coupling is a very appealing feature which enables those systems to possess a very long-lived excited state, each time a light excitation of the Ru^{2+} center takes place and subsequent energy transfer to the Os^{2+} center or electron transfer to the oxidized Os^{3+} center occurs. Such a long excited state can then be used for further chemical reactions, e.g., redox reactions in artificial photosynthesis, water splitting, and other important processes.

In this work we intend to extend the lifetime of the Ru−PAP−Os excited state even further. To explain how we intend to do that, let us consider the following cases. If we place acceptor ligands (L = A in Figure 1) on the Ru^{2+} center of Ru^{2+}−PAP−Os^{2+}, upon light excitation the excited state will be strongly localized on A and then energy transfer to the Os^{2+} center will occur. If we place acceptor ligands (A) on the Ru^{2+}

(1) See, for example: Hader, D.-P.; Tevini, M. *General Photobiology*; Pergamon: Oxford, England, 1987.
(2) (a) Fox, M. A.; Chanon, M. *Photoinduced Electron Transfer*; Elsevier: New York, 1988. (b) Mattay J. *Top. Curr. Chem.* **1990**, 156; **1991**, 159.
(3) Demas, J. N.; Adamson, A. W. *J. Am. Chem. Soc.* **1971**, *93*, 1800.
(4) (a) Lehn, J.-M. *Angew. Chem. Int. Ed. Engl.* **1988**, *27*, 89. (b) Cram, D. J. *Angew. Chem., Int. Ed. Engl.* **1988**, *27*, 1009. (c) Kohnke, F. H.; Mathias, J. P.; Stoddard, J. F. *Angew. Chem. Int. Ed. Engl. Adv. Mater.* **1989**, *28*, 1103.
(5) Scandola, F.; Indelli, M.-T.; Chiorboli, C.; Bignozzi, C. A. *Top. Curr. Chem.* **1990**, *158*, 73.
(6) (a) Balzani, V. *Supramolecular Photochemistry*; Reidel: Dordrecht, The Netherlands, 1987. (b) Balzani, V.; Scandola, F. *Supramolecular Photochemistry*; Horwood: Chichester, U.K., 1991.
(7) See, for example: (a) Sauvage, J.-P.; Collin, J.-P.; Chambron, J.-C.; et al. *Chem. Rev.* **1994**, *94*, 1993. (b) Barigelletti, F.; Flamigni, L. *Chem. Soc. Rev.* **2000**, *29*, 1.
(8) (a) Crosby, G. A.; Watts, R. J.; Carsten, D. H. *Science* **1970**, *170*, 1195. (b) Meyer, T. J. *Pure Appl. Chem.* **1986**, *58*, 1193. (c) Juris, A.; Balzani, V.; Barigelletti, F.; Campagna, S.; Belser, P.; von Zelewsky, A. *Coord. Chem. Rev.* **1988**, *84*, 85. (d) Kalyanasundaram, K. *Photochemistry of Polypyridine and Porphyrin Complexes*; Academic Press: London, U.K., 1992.
(9) (a) Collin, J.-P.; Harriman, A.; Heitz, V.; Odobel, F.; Sauvage, J.-P. *Coord. Chem. Rev.* **1996**, *148*, 63. (b) De Cola, L.; Belser, P. *Coord. Chem. Rev.* **1998**, *177*, 301.
(10) (a) De Cola, L.; Balzani, V.; Barigelletti, F.; Flamigni, L.; Belser, P.; Bernhard, S. *Rec. Trav. Chim. Pays-Bas* **1995**, *114*, 534. (b) Balzani, V.; Barigelletti, F.; Belser, P.; Bernhard, S.; De Cola, L.; Flamigni, L. *J. Phys. Chem.* **1996**, *100*, 16786.
(11) Bernhard, S.; Belser, P. *Synthesis* **1996**, 192.

10.1021/ic000694c CCC: $20.00
Published on Web 02/21/2001

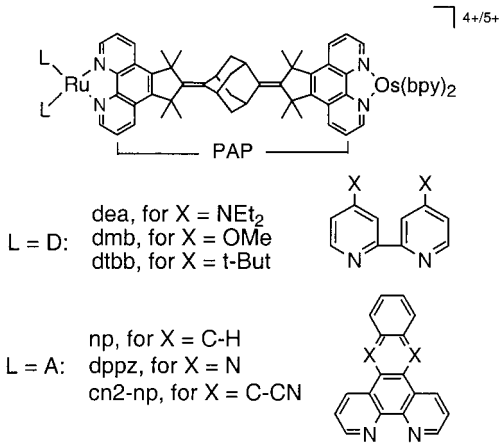

Figure 1. Ru−PAP−Os complex, where L is a bpy ligand, an acceptor (A), or donor (D) ligand. Donor ligands (L = D): 4,4′-bis(diethylamino)-2,2′-bipyridyl (dea), 4,4′-dimethoxy[2,2′]bipyridinyl (dmb), 4.4′-di-*tert*-butyl[2,2′]bipyridinyl (dtbb); and acceptor ligands (L = A): naphtho[2,3-*f*][1,ω]phenanthroline (np), dipyrido[3,2-*a*:2′,3′-*c*]phenazine (dppz), and naphtho[2,3-*f*][1,ω]phenanthroline-9,14-dicarbonitrile (cn2-np).

center of Ru^{2+}−PAP−Os^{3+}, the excited electron of Ru^{3+}−$A^{\bullet-}$ will be strongly stabilized by the acceptor ligand and then transferred to the Os^{3+} center. Moreover, if we put donor ligands (L = D in Figure 1) on the Ru^{2+} center of Ru^{2+}−PAP−Os^{3+}, the excited electron will be localized on the phen (Ru^{3+}−$phen^{\bullet-}$), which has lower π^* orbitals with respect to those of a donor ligand, and then transferred to the Os^{3+} center. The latter will be reduced to Os^{2+}, and the oxidized Ru^{3+} center will be stabilized by the D ligands (D^+−Ru^{2+}). In each case the excited state will be stabilized and its lifetime prolongated. However, these systems are difficult to synthesize.[9b] Thus an initial theoretical study is carried out in order to predict the donor and acceptor character of a series of potential ligands. The result of these computer simulations will help us to select the best D and A ligands and improve the electron/energy-transfer processes in the Ru−PAP−Os dyad. Such a prediction would reduce the preparative work to nothing but the best predicted system.

Density functional calculations[12] are best suited for investigating such big systems containing heavy metals such as Ru and Os. Furthermore, since the two chelating phen units of PAP are not communicating with each other, calculations can be restrained to the monomeric metal units $Ru(A)_2(phen)^{2+}$ and $Ru(D)_2(phen)^{2+}$. The ligands that have been chosen as donor (D) and acceptor (A) are reported in Figure 1.

Experimental Section

(i) Chemicals. For the cn2-np*'s* synthesis, *o*-xylylene dicyanide was obtained by commercial sources (Fluka, assay > 97%) and 1,10-phenanthroline-5,6-dione was prepared according to literature procedures.[13] 1,10-Phenanthroline monohydrate (Phen × H_2O) and NH_4PF_6 were purchased from Fluka, and $RuCl_3 \times 3H_2O$ from JM (assay 41.80%). All solvents used in the preparations were reagent grade and used as supplied. Silica gel preparative plates and/or aluminum oxide chromatographic columns were used for purification of the metal complexes. The preparative SiO_2 plates were made of silica gel purchased from Merck (60, particle size 0.040−0.063 mm) and prepared according to the procedure indicated by Merck. Aluminum oxide for chromatography was purchased from Fluka (type 507 C neutral, Brockmann grade I, particle size 0.05−0.15 mm, pH 7.0 ± 0.5).

(ii) Analytical Methods. ^{1}H NMR spectra were recorded with a Varian Gemini-300 spectrometer (300.075 MHz), and chemical shifts are given in ppm using the solvent itself as internal standard. ESI (electron spray ionization) mass spectra were measured with a Bruker FTMS 4.7 T Bio APEXII.

(iii) Synthesis. (a) Ligands. Literature procedures were used for the syntheses of the ligands dea,[14a] dmb,[14b] dtbb,[14c] dppz,[14d] cn2-np and np[15](for the ligand abbreviations, see Figure 1).

(b) Metal Precursors. The Ru(II) precursors of the type $RuL_2Cl_2 \times nH_2O$ (where L = dmb, dtbb, cn2-np, dppz) were prepared following the method described for the synthesis of $Ru(bpy)_2Cl_2 \times 2H_2O$.[16] $[Ru(dea)_2Cl_2]Cl$ was prepared according to literature methods.[14a]

(c) $[Ru(dea)_2(phen)](PF_6)_2$. Phen × H_2O (75 mg, 0.38 mmol), $[Ru(dea)_2Cl_2]Cl \times 4H_2O$ (87 mg, 0.1 mmol), and NEt_3 (0.4 mmol, 2 mmol) were heated at 110 °C in 100 mL of 50% ethanol/water under Ar for 4 h. The ethanol was removed under reduced pressure, NH_4PF_6 (2 g) was added, and the resulting red precipitate was isolated by suction filtration. The crude product was purified on a column of neutral aluminum oxide (2 × 12 cm) with 1:2 acetonitrile/toluene as eluent. The first red band (TLC: $R_f = 0.8$, support SiO_2, solvent acetonitrile/toluene, 1:2) was isolated, the solvent was removed under reduced pressure, and the product obtained was further purified on SiO_2 plates ($MeCN/H_2O$/t-BuOH/KNO_3, 4:1:1:0.1, as eluent). Yield: 56%. MS/ESI: *m*/*z* 1023 ($M^+ - PF_6$; calcd 1023). ^{1}H NMR (300 MHz, CD_3CN): δ 8.46 (d, 2H), 8.28 (d, 2H), 8.16 (s, 2H), 7.71 (dd, 2H), 7.42 (d, 2H), 7.35 (d, 2H), 7.33 (d, 2H), 6.77 (d, 2H), 6.64 (2d, 2H), 6.26 (2d, 2H), 3.55 (q, 8H), 3.43 (q, 8H), 1.20 (t, 12H), 1.10 (t, 12H).

(d) $[Ru(dppz)_2(phen)](PF_6)_2$. Phen × H_2O (25 mg, 0.12 mmol) and $Ru(dppz)_2Cl_2 \times 2H_2O$ (97 mg, 0.12 mmol) were suspended in ethylene glycol (3 mL) with 5% water content and heated at 150 ° C under Ar for 13 h. The solvent was removed under reduced pressure, then water (10 mL) and NH_4PF_6 (2 g) were added to give a red precipitate, which was separated by suction filtration. The crude product was purified on a column of neutral aluminum oxide (7 × 2 cm) with acetone as eluent. The first orange band (TLC: $R_f = 0.8$, support SiO_2, solvent MeCN/H_2O/t-MeOH/KNO_3, 4:1:1:0.1) was isolated, the solvent was removed under reduced pressure, and the product obtained was further purified on SiO_2 plates ($MeCN/H_2O$/t-BuOH/KNO_3, 4:1:1:0.1, as eluent). Other solvent mixtures have been used for the purification by plates: MeCN/$MeNO_2$/H_2O/KNO_3, 4:0.2:1:0.1, 4:0.5:1:0.1; DMF/H_2O/NH_4Cl, 4:1:0.1, 2:1:0.1; but the best separation is obtained with $MeCN/H_2O$/t-BuOH/KNO_3, 4:1:1:0.1. The isolation of the orange band with $R_f = 0.6$ gave 30% of pure product. MS/ESI: *m*/*z* 991 ($M^+ - PF_6$; calcd 991); ^{1}H NMR (300 MHz, CD_3CN): δ 9.64 (d, 2H), 9.62 (d, 2H), 8.65 (d, 2H), 8.5−8.4 (m, 4H), 8.31 (d, 2H), 8.29 (s, 2H), 8.23 (d, 2H), 8.15−8.09 (m, 6H), 7.83−7.75 (2dd, 4H), 7.69 (dd, 2H).

(e) $[Ru(cn2\text{-}np)_2(phen)](PF_6)_2$. Phen × H_2O (10 mg, 0.05 mmol) and $Ru(cn2\text{-}np)_2Cl_2$ (42 mg, 0.05 mmol) were suspended in ethylene glycol (2 mL) with 5% water content and were heated to 150 °C under Ar for 12 h. The solvent was removed under reduced pressure, and water (10 mL) and NH_4PF_6 were added to give a red precipitate, which was isolated by suction filtration (61 mg, 39% yield). The crude product was dissolved in acetone (6 mL) and purified on a column of neutral aluminum oxide (12 × 2 cm) with acetone as eluent. The first yellow band (TLC: $R_f = 0.6$, support SiO_2, solvent MeCN/$MeNO_2$/H_2O/KNO_3, 4:0.2:1:0.1) was eliminated. Then, the second orange band was isolated (TLC: $R_f = 0.5$, support SiO_2, solvent MeCN/$MeNO_2$/H_2O/KNO_3, 4:0.2:1:0.1) using acetone containing 1% water as eluent. The solvent was then removed, and the product obtained was further purified on

(12) See, for example: (a) Parr, R. G.; Yang, W. *Density-Functional Theory of Atoms and Molecules*; Oxford University Press: New York, 1989. (b) Daul, C. A.; Doclo, K. G.; Stückl, A. C. *On the Calculation of Multiplets* in *Recent Advances in Density Functional Methods (Part II)*; World Scientific Publishing: Singapore, 1997.

(13) Yamada, M.; Tanaka, Y.; Yoshimoto, Y *Bull. Chem. Soc. Jpn.* **1992**, *65*, 1006.

(14) (a) Slattery, S. J.; Gokaldas, N.; Mick, T.; Goldsby, K. A. *Inorg. Chem.* **1994**, *33*, 3621. (b) Maerker, G.; Case, H. F. **1958**, *80*, 2745. (c) Belser, P.; von Zelewsky, A. *Helv. Chim. Acta*, **1980**, *63*, 1675. (d) Dickeson, J. E.; Summers, L. A. *Aust. J. Chem.* **1970**, *23*, 1023.

(15) Albano, G.; Belser, P.; De Cola, L.; Gandolfi, M.-T. *Chem. Commun.* **1999**, 1171.

(16) Sullivan, B. P.; Salmon, D. J.; Meyer T. J. *Inorg. Chem.* **1978**, *17*, 3334.

SiO_2 plates with MeCN/H_2O/t-ButOH/KNO_3, 4:1:1:0.1, as eluent. Yield: 3%. MS/ESI: *m/z* 991 ($M^+ - PF_6$; calcd 991). ^{1}H NMR (300 MHz, CD_3 CN): δ 10.04 (d, 2H), 10.01 (d, 2H), 8.77 (m, 4H), 8.65 (d, 2H), 8.29 (s, 2H), 8.24 (d, 2H), 8.21−8.16 (m, 6H), 8.06 (d, 2H), 7.82 (dd, 2H), 7.75 (dd, 2H), 7.70 (dd, 2H).

(f) [Ru(dtbb)$_2$(phen)](PF$_6$)$_2$. Phen × H_2O (25 mg, 0.12 mmol) and $Ru(dtbb)_2Cl_2$ (89 mg, 0.12 mmol) were suspended in ethylene glycol (2 mL) with 5% water content and were heated in the microwave oven for 3 × 2 min. The solvent was removed under reduced pressure, and the residue was dissolved in water (10 mL). NH_4PF_6 (2 g) was added to the aqueous solution to give a red precipitate, which was isolated by suction filtration. The crude product (150 mg, 97% yield) was dissolved in acetone (4 mL) and purified on a silica column (Kieselgel 60, 230−400 mesh ASTM, 10 × 3 cm) with acetone as stationary phase and with MeCN/H_2O/t-ButOH/KNO_3, 4:1:1:0.1, as eluent. The second orange band from the bottom ($R_f = 0.9$) was isolated and the solvent removed under reduced pressure. Yield: 72%. MS/ESI: *m/z* 991 ($M^+ - PF_6$; calcd 991). ^{1}H NMR (300 MHz, CD_3 CN): δ 8.59 (d, 2H), 8.50 (d, 2H), 8.45 (d, 2H), 8.22 (s, 2H), 8.04 (d, 2H), 7.74 (dd, 2H), 7.68 (d, 2H), 7.44 (2d, 2H), 7.38 (d, 2H), 7.18 (2d, 2H), 1.43 (s, 18H), 1.34 (s, 18H).

(g) [Ru(dmb)$_2$(phen)](PF$_6$)$_2$. Phen × H_2O (14 mg, 0.07 mmol) and $Ru(dmb)_2Cl_2$ (45 mg, 0.07 mmol) were suspended in ethylene glycol (2 mL) with 5% water content and were heated in a microwave oven for 3 × 2 min. The solvent was removed under reduced pressure. Water (10 mL) and NH_4PF_6 (2 g) were added to give an orange precipitate, which was isolated by suction filtration. The crude product was purified on SiO_2 plates (MeCN/H_2O/t-ButOH/KNO_3, 4:1:1:0.1) as eluent. Yield: 20%. MS/ESI: *m/z* 858 ($M^+ - PF_6$; calcd 858). ^{1}H NMR (300 MHz, CD_3 CN): δ 8.56 (d, 2H), 8.21 (s, 2H), 8.15 (d, 2H), 8.03 (d, 2H), 7.98 (d, 2H), 7.72 (dd, 2H), 7.65 (d, 2H), 7.23 (d, 2H), 7.02 (dd, 2H), 6.73 (dd, 2H), 6.74−6.71 (m, 2H).

(iv) Photophysics. Absorption spectra were recorded using a Perkin-Elmer UV−visible spectrophotometer Lambda 40. Luminescence measurements were made using a Perkin-Elmer fluorescence spectrophotometer LS 50B exciting in the MLCT transition of the Ru(II) complex. Quantum yields of luminescence at room temperature were calculated according to literature procedures,[17] using an aerated aqueous solution of $[Ru(bpy)_3]^{2+}$ as a standard ($\phi_{em} = 0.028$).[18] Spectrophotometric grade acetonitrile (Fluka) was used for all spectroscopic measurements.

(v) Computational Methods. The density functional calculations reported in this work have been carried out with the Amsterdam Density Functional (ADF) program package.[19] The computational scheme is characterized by a density fitting procedure to obtain the Coulomb potential[19a] and by elaborate 3D numerical integration techniques[19b,c] for the evaluation of the Hamiltonian matrix elements, including those of the exchange−correlation energy and potential. Local density approximation (LDA) was applied with the X_α functional for the exchange[20] and the Vosko−Wilk−Nuisar functional[21] for the correlation potential. The frozen core (FC) approximation for the inner core electrons was used for all atoms. The orbitals up to 3d for Ru and 1s for N and C atoms were kept frozen. Valence electrons of C atoms were treated with double-ζ basis functions and those of N atoms with triple-ζ basis functions, and hydrogens were treated with a single-ζ function. For carbon and nitrogen atoms a single-ζ polarization function was added to the basis set. Valence electrons of Ru were treated with triple-ζ basis functions except the 4s orbital, which was expanded in a double-ζ basis. A single-ζ 5p polarization function was added. A geometry optimization of all systems was performed in internal coordinates using the Broyden−Fletcher−Goldfarb−Shanno algorithm[22] to update the Hessian matrix. Complete geometry optimization was performed imposing a C_{2v} symmetry to the free ligands, except in the case of dea, where the symmetry was kept to C_s, and a C_2 symmetry to the complexes, except in the case of $Ru(dea)_2(phen)^{2+}$, where the symmetry C_s was used.

Table 1. Spectroscopic Properties of $[Ru(L)_2(phen)]^{2+}$ in CH_3CN at 298 K

L	λ_{max}^{abs} (10^{-4} ϵ)[a]	λ_{max}^{em}	10^{-3} ϕ_{em}
deab	475 (1.40)	754	0.5
dmb	462 (1.31)	640	4.6
dtbb	453 (1.45)	615	6.3
bpy	447 (1.53)[b]	600c	
dppz	448 (1.84)	611	28
cn2-np	427 (1.64)	664	0.4

[a] Maximum of the MLCT absorption band in the visible. [b] Ref 26. [c] In CH_2Cl_2, ref 27.

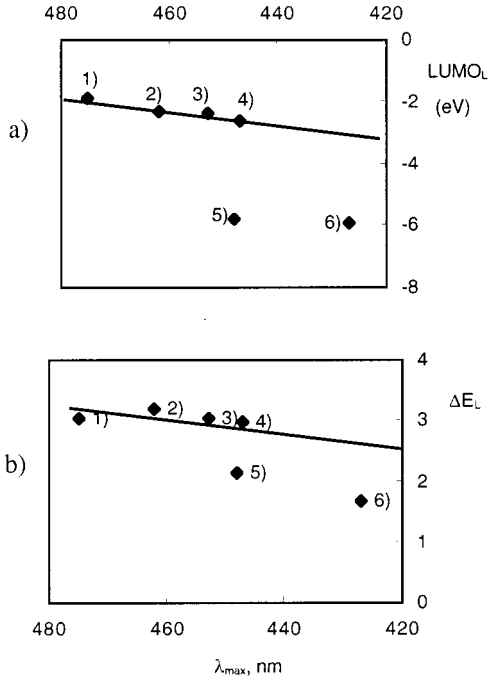

Figure 2. (a) LUMO of the free ligands vs the MLCT absorption band in the visible of $Ru(L)_2(phen)^{2+}$, where L = (1) dea, (2) dmb, (3) dtbb, (4) bpy, (5) dppz, (6) cn2-np. (b) ΔE(HOMO−LUMO) of the free ligands L vs the MLCT absorption band in the visible of the $Ru(L)_2(phen)^{2+}$ with L as above.

Results

The photophysical properties of all complexes are reported in Table 1. We can correlate the calculations performed on the free ligands with the experimental data of their Ru(II) complexes by plotting the energy of the MLCT band in the visible vs the following: (1) the energy of the calculated LUMO (Figure 2a), and (2) the difference in energy between the HOMO and the LUMO (Figure 2b) of the free ligands.

Ligands' MOs. To determine the σ-donor and π*-acceptor capability of the chosen ligands, the corresponding molecular orbitals were calculated. The calculations were performed for the geometry optimized with the ADF program (C═N 1.33 Å, C═C 1.38 Å). The calculated energies of the HOMO and the LUMO for the different ligands are reported in Figure 3. The

(17) Demas, J. N.; Crosby, G. A. *J. Phys. Chem.* **1980**, *84*, 2068.
(18) Allen, G. H.; White, R. P.; Rillema, D. P.; Meyer, T. J. *J. Am. Chem. Soc.* **1982**, *104*, 4803.
(19) (a) Baerends, E. J.; Ellis, D. E.; Ross, P. *Chem. Phys.* **1993**, *2*, 42. (b) Boerrigter, P. M.; te Velde, G.; Baerends, E. J. *Int. J. Quantum Chem.* **1988**, *33*, 87. (c) te Velde, G.; Baerends, E. J. *J. Comput. Phys.* **1992**, *99*, 84.
(20) Slater, J. C. *Quantum Theory of Molecules and Solids*, Vol. 4: *Self-Consistent Field for Molecules and Solids*; McGraw-Hill: New York, 1974.
(21) Vosko, S. H.; Wilk, L.; Nuisar, M. *Can. J. Phys.* **1980**, *58*, 1200.
(22) Press: W. H.; Flannery, B. P.; Teukolsky, S. A.; Vetterling, W. T. *Numerical Recipes*; Cambridge University Press: Cambridge, UK, 1989.

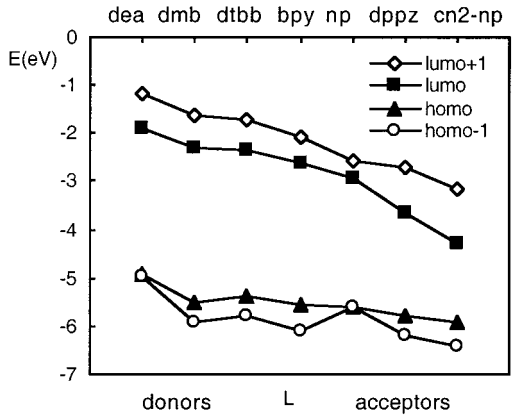

Figure 3. Energy plot of the ligands' molecular orbitals.

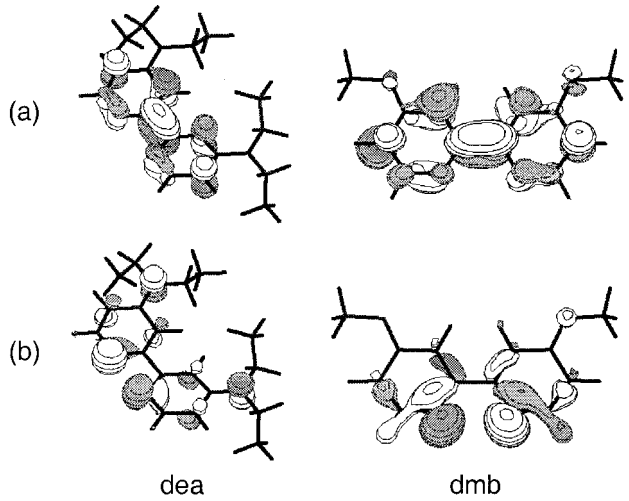

Figure 4. LUMO (a) and HOMO (b) of dea compared to those of dmb.

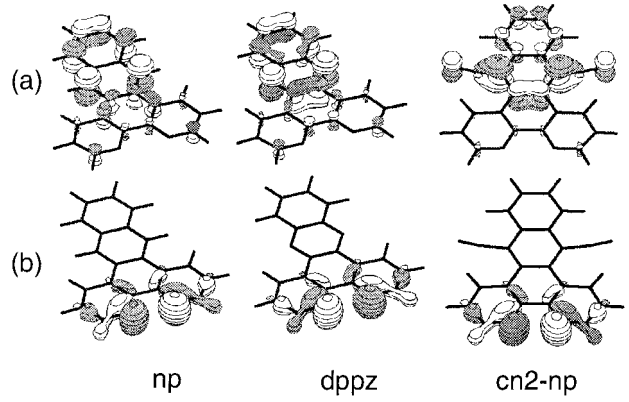

Figure 5. LUMO (a) and HOMO (b) of the acceptor ligands np, dppz, and cn2-np.

calculated electronic density of the HOMO and the LUMO are shown in Figure 4 for two (dea, dmb) of the donor ligands, and in Figure 5 for the acceptor ligands (cn2-np, dppz, np).

Metal Complexes' MOs. To determine if the electron involved in the MLCT transition will be localized on the external ligands L or on the phen unit of the bridging ligand, a simple calculation of the orbital energies for the free ligands is not sufficient. Indeed, the $HOMO_M$ centered on the metal must also be taken into account as well as the energy of the $LUMO_L$ centered on the ligand, which will be different from the LUMO's energy of the free ligand. Therefore, calculations of the MOs of the whole $Ru(L)_2(phen)^{2+}$ complexes were performed, starting from a geometry optimization of each complex (Ru−N 2.05 Å, C═N 1.35 Å, C═C 1.38 Å). The calculated electronic densities of the LUMO are reported in Figure 6 for two complexes with acceptor ligands (cn2-np, dppz) and for one complex with a donor ligand (dea).

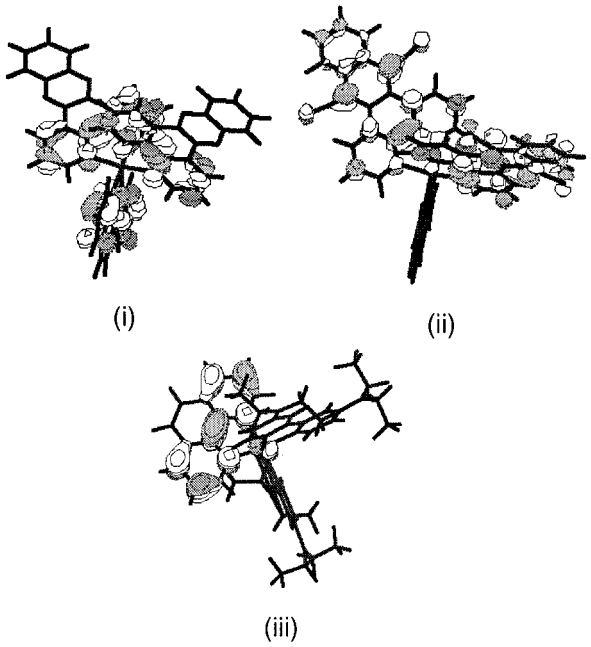

Figure 6. LUMO of $Ru(L)_2(phen)^{2+}$, where L = (i) cn2-np, (ii) dppz, and (iii) dea.

4. Discussion

(a) General. Absorption of visible light by a Ru(II)−BL−Os(II) (BL bridging ligand) dinuclear complex causes excitation of the Ru center from the singlet ground state to the lowest ^{1}MLCT excited state. This ^{1}MLCT excited state undergoes nonradiative deactivation (intersystem crossing: ISC) to the lowest ^{3}MLCT excited state ($\eta_{isc} = 1$). Energy or electron transfer can then occur to the lowest ^{3}MLCT excited state of the Os(II) or Os(III) center, respectively. The properties of the ^{1}MLCT and ^{3}MLCT excited states of the Ru(II) center can be tuned by a judicious choice and combination of ligands (see refs 8c and 23). More precisely, the energies of the MLCT excited states depend on the following physicochemical properties: (1) the reduction potential of the ligand involved in the MLCT transition, (2) the oxidation potential of the metal in the complex, which is affected by the electron σ-donor and π-acceptor properties of all ligands, and (3) the charge separation caused by the transition (Ru → L); that is, the Coulombic interaction between the hole on the metal and the electron on the ligand decreases with increasing separation distance M−L.

Big changes of the energy of the excited states can be obtained by changing the ligand involved in the MLCT transition. This occurs in the case of $Ru(cn2\text{-}np)_2(phen)^{2+}$, $Ru(dppz)_2(phen)^{2+}$, and $Ru(np)_2(phen)^{2+}$, while smaller changes are observed when substituting the 4 and 4′ positions of the bpy ligands (case of L = dea, dmb, dtbb in $Ru(L)_2(phen)^{2+}$).

(b) Acceptor Ligands. The acceptor ligands that have been chosen, i.e., cn2-np, np, and dppz, are known to show a very

(23) Johnson, S. R.; Westmoreland, T. D.; Caspar, J. V.; Barqawi, K. R.; Meyer, T. J. *Inorg. Chem.* **1988**, *27*, 3195, and references therein.

peculiar character.[15,24] Indeed, they can be thought to be made of a bpy chelate with an extended anthracenic-like π system appended to it. Electrochemical measurements strongly support this hypothetical electronic separation between the two subunits.[15,24] From the calculated orbital contours (see Figure 5), it can be noticed that despite the large aromatic system anchored to the bpy unit, the HOMO is still strongly localized on the N of the bpy moiety; therefore the ligand has also a strong σ-donor character. On the other hand, the LUMO is strongly localized on the π-accepting anthracenic unit. Therefore, the DF calculations confirm the hypothesis, based on the electrochemical measurements, of an electronic separation between the bpy subunit and the anthracenic one.

(c) Ru(II) Complexes with Acceptor Ligands. The acceptor ligands here under study show experimentally a peculiar behavior also when they are coordinated to a Ru(II) metal center.[15,24] In the case of $Ru(dppz)_2(phen)^{2+}$ the absorption band in the visible is very similar in energy (see Table 1) and shape to that of $Ru(bpy)_2(phen)^{2+}$. Thus, the MLCT band in the visible is unexpectedly not affected by the presence of the acceptor phenazine moieties. On the other hand, in $Ru(cn2\text{-}np)_2(phen)^{2+}$ a perturbation of the $Ru(bpy)_2(phen)^{2+}$ kernel can be observed as a broadening of the MLCT band in the visible. Indeed, even if the absorption maximum in the visible occurs at the same energy as in $Ru(bpy)_2(phen)^{2+}$ (see Table 1), the corresponding band is much larger and extends in the red. This broadening effect is due to the sum of different bands, corresponding to absorption to at least two different MLCT excited state, one involving the phen ligand at higher energy (maximum of the absorption band) and one involving the cn2-np ligands at lower energy (broadening of the absorption band around 480 nm). DF calculations confirm the experimental data. Indeed, if we look at the calculated $LUMO_L$ of the complexes in Figure 6, (i) and (ii), we can see that the $LUMO_L$ of $Ru(dppz)_2(phen)^{2+}$ is localized on the phen ligand and the bpy part of the dppz ligands, while the $LUMO_L$ of $Ru(cn2\text{-}np)_2(phen)^{2+}$ is localized on the cn2-np ligands. This result is also in agreement with an electron-acceptor character increasing from dppz to cn2-np. Furthermore, from the plots shown in Figure 2a,b, it can be noticed that $Ru(cn2\text{-}np)_2(phen)^{2+}$ and $Ru(dppz)_2(phen)^{2+}$ lie far away from the straight line correlating the points corresponding to the other complexes. This is in agreement with the fact that, even if the LUMO of the free accepting ligands is very low in energy with respect to bpy, the complexes show an absorption maximum in the visible at almost the same energy as $Ru(bpy)_2(phen)^{2+}$.

The presence of two MLCT excited states within $Ru(cn2\text{-}np)_2(phen)^{2+}$ is observed also in emission. For example, (cn2-np)-based complexes show an exceptionally long lifetime of the excited state and two very weak emission bands. Observation of two emission bands coming from the same complex was explained by the presence of two nonequilibrated ^{3}MLCT excited states, one involving the cn2-np and one involving the external bpy (or phen) ligands.[15] Furthermore, a nonemitting ^{3}IL (intraligand) excited state centered on the dicarbonitrile−anthracene unit, which is lower in energy, is responsible for the very long lifetime of the excited state (for more details see ref 15). From the previous discussion, it becomes evident that the cn2-np ligand is the best candidate as acceptor for the electron/energy-transfer processes within PAP-based dinuclear complexes. Indeed, the experimental and calculated properties for its Ru(II) complex show that the electron, excited upon irradiation, is transferred to the dicarbonitrile−anthracene units, in particular to the ring substituted with the CN groups, in agreement with a strong electron-acceptor character of the CN groups. Such an IL excited state lives long enough to give rise to energy/electron transfer to the Os(II/III) center, since the ^{3}IL of the coordinated cn2-np is still higher in energy with respect to the ^{3}MLCT of the $Os(bpy)_2(phen)^{2+}$ unit. To summarize, (1) $Ru(cn2\text{-}np)_2(phen)^{2+}$ shows an absorption maximum close to that of $Ru(bpy)_2(phen)^{2+}$, (2) upon absorption of a photon, the excited electron is preferentially localized on cn2-np rather than on the phen part of the bridging ligand, and (3) the excited electron stays for a relatively long time on the anthracenic unit of cn2-np.

(d) Donor Ligands. From Figure 3 it can be noticed that the energy of the LUMO decreases with increasing acceptor character of the ligands. Furthermore, the energy difference between the HOMO and the LUMO decreases when going from the donors to the acceptors, as expected on the basis of the general discussion. However, a slight discrepancy can be noticed in the case of the donor ligands dea and dmb. The dea ligand shows a higher LUMO energy, while dmb has a HOMO lying at lower energy. Consequently, the energy difference (ΔE) between HOMO and LUMO is larger for dmb even though dea is expected to be a stronger donor than dmb after comparison with the corresponding benzene-substituted derivatives, *N*,*N*-diethylanyline and methoxybenzene, respectively. This discrepancy can be explained by looking at the orbital contours (see Figure 5). Indeed, it can be noticed that the LUMO of dmb is partially delocalized, and hence stabilized, on the oxygen atoms, while the LUMO of dea is localized only on the aromatic rings of bpy. On the other hand, the HOMO of dea is delocalized on the nitrogen atoms of the substituents, whereas in dmb the electronic density is strongly localized on the nitrogen atoms of the bpy unit. In conclusion the dmb is both a stronger π*-acceptor and a stronger σ-donor with respect to dea. Finally, the dtbb has electronic properties very similar to those of the unsubstituted bpy, showing a slight donor character owing to the well-known I^+ effect observed for alkyl substituents on aromatic rings.

(e) Ru(II) Complexes with Donor Ligands. The calculations carried out for the free donor ligands are in agreement with the absorption properties of their Ru(II) complexes (see Table 1). Indeed, the absorption maximum in the visible for the dea complex lies at lower energy (475 nm) with respect to the analogous dmb complex (462 nm), and the dtbb complex absorbs (453 nm) very near the bpy complex (450 nm). Furthermore, the MOs of the Ru(II) complexes with the donor ligands were calculated. The $LUMO_L$ is centered on the phen ligand, rather than on the peripheral donor ligands. An example of $LUMO_L$ is reported in Figure 6, (iii) for L = dea. In conclusion, in the case of the donor ligands, dmb seems to be the best candidate. It is a strong σ-donor, so that the electron promoted upon visible-light excitation is transferred preferentially to the phen part of the bridging ligand, rather than to the external dmb ligands and for the same reason dmb stabilizes the Ru(III) center much better than dea. At the same time, the dmb complex shows an absorption maximum (462 nm), which

(24) (a) Chambron, J.-C.; Sauvage, J.-P.; Amouyal, E.; Koffi, P. *New J. Chem.* **1985**, *9*, 527. (b) Amouyal, E.; Homsi, A.; Chambron, J.-C.; Sauvage, J.-P. *J. Chem. Soc., Dalton Trans.* **1990**, *1990*, 1841. (c) Olson, E. J. C.; Hu, D.; Hoermann, A.; Jonkman, A. M.; Arkin, M. R.; Stemp, E. D. A.; Barton, J. K.; Barbara, P. F. *J. Am. Chem. Soc.* **1997**, *119*, 11458. (d) Baba, A. I.; Shaw, J. R.; Simon, J. A.; Thummel, R. P.; Schmehl, R. H. *Coord. Chem. Rev.* **1998**, *171*, 43.

(25) Opperman, K. A.; Macklenburg, S. L.; Meyer, T. J. *Inorg. Chem.* **1994**, *33*, 5295.

(26) Belser, P.; von Zelewsky, A. *Helv. Chim. Acta* **1980**, *63*, 1675.

(27) Caspar, J. V.; Meyer, T. J. *Inorg. Chem.* **1980**, *63*, 2444.

is less red-shifted than the dea complex (475 nm), with respect to the prototype $Ru(bpy)_2(phen)^{2+}$ (447 nm). Indeed the energy of the ^{1}MLCT and consequently of the ^{3}MLCT level of the Ru(II) center (640 nm for $Ru(dmb)_2(phen)^{+2}$, 754 nm for $Ru(dea)_2(phen)^{2+}$) should not become lower than that of the ^{3}MLCT level of the Os(II) acceptor unit (743 nm for $Os(bpy)_2(phen)^{+2}$). An ideal donor ligand would be a donor equivalent to cn2-np for the acceptor series, i.e., a ligand showing the same absorption properties as bpy in the Ru complex, but with an appended donor unit, capable of stabilizing the Ru(III) center formed upon the light excitation process. The bpy-PTZ ({10-[(4′-methyl-2,2′-bipyridin-4-yl)methyl]phenothiazine}) and its analogues seem to show such a behavior.[15] Calculations on bpy-PTZ and its Ru(II) complex are on the way.

5. Conclusions

From the above discussion, it comes in evidence that donor and acceptor ligands with a bpy-type kernel and an appended donor or acceptor site are the most suitable ones for improving energy- and electron-transfer processes in dinuclear complexes of Ru(II) and Os(II/III) linked by rigid rod-like bridging ligands (e.g., PAP). This result can be extended to all polynuclear systems, where electronic coupling between the metal units is very weak. Furthermore we have demonstrated that the computational method used in this work can be exploited for the classification of metal-coordinated polypyridine ligands as acceptors or donors, with respect to the coordinated phen.

Acknowledgment. We wish to thank the Swiss National Science Foundation for financial support.

IC000694C